

Iris Recognition Based On the Low Order Norms of Gradient Components

Iman A. Saad, Loay E. George

Abstract—Iris pattern is an important biological feature of human body; it becomes very hot topic in both research and practical applications. In this paper, an algorithm is proposed for iris recognition and a simple, efficient and fast method is introduced to extract a set of discriminatory features using first order gradient operator applied on grayscale images. The gradient based features are robust, up to certain extents, against the variations may occur in contrast or brightness of iris image samples; the variations are mostly occur due lightening differences and camera changes. At first, the iris region is located, after that it is remapped to a rectangular area of size 360x60 pixels. Also, a new method is proposed for detecting eyelash and eyelid points; it depends on making image statistical analysis, to mark the eyelash and eyelid as a noise points. In order to cover the features localization (variation), the rectangular iris image is partitioned into N overlapped sub-images (blocks); then from each block a set of different average directional gradient densities values is calculated to be used as texture features vector. The applied gradient operators are taken along the horizontal, vertical and diagonal directions. The low order norms of gradient components were used to establish the feature vector. Euclidean distance based classifier was used as a matching metric for determining the degree of similarity between the features vector extracted from the tested iris image and template features vectors stored in the database. Experimental tests were performed using 2639 iris images from CASIA V4-Interval database, the attained recognition accuracy has reached up to 99.92%.

Keywords—Iris recognition, contrast stretching, gradient features, texture features, Euclidean metric.

I. INTRODUCTION

BIOMETRICS is the study of behavioral or physical characteristics of human including items such as finger prints, face, hand geometry, voice and iris. Among the biometrics, iris has highly accurate and reliable characteristics. An iris has unique structure and it remains stable over a person life time, which is observed through the clinical evidence [1]. The created iris patterns of human are largely completed at the eighth month after his born. Pigment accretion can continue into the first postnatal year. Formation of unique iris patterns is random and not related to any genetic factor. Due to the epigenetic nature of iris, two eyes of an individual contain completely independent iris patterns. Iris has unique features and highly complex patterns to be used as a biometric [2], [3], therefore, the iris recognition systems are very reliable and could be used in most secure places [4], [5]. Many feature extraction algorithms have been developed in the literature;

Iman A. Saad is with the Electronic Computer Center, University of Mustansiriyah, Baghdad, Iraq (e-mail: eman_abduljabbar@yahoo.com).

Dr. Loay E. George works with the Department of Computer Science, College of Science, University of Baghdad, Baghdad, Iraq (e-mail: loayedwar57@yahoo.com).

they differ either in the iris feature representations or in the pattern matching algorithms.

Most of the studies concentrated on extracting texture feature information from iris region, such that they contain inherent characteristics of the iris that are essential to iris recognition. Daugman [6] made use of two-dimensional Gabor filters to demodulate texture phase structure information of the iris, use the result to get the iris texture characteristics of the local phase, and then to the match, the difference between a pair of iris codes was measured by their Hamming distance. After Daugman work, many scholars proposed a variety of iris recognition methods. Boles and Boashah introduced an algorithm for iris recognition based on the wavelet transform zero crossing detection; they calculated zero-crossing representation of 1D wavelet transform at various resolution levels of a virtual concentric circle on an iris image to characterize the texture of the iris image. Monro [7] developed an iris coding method based on DCT for feature extraction. He used Iris images obtained from CASIA database, version 1 and the Bath database. Azizi and Pourreza [8] proposed a set of local and global properties of an iris image for establishing iris feature vector. Also, some sets of local binary features based on Haar wavelet [9]. Sarhan [10] used discrete cosine transform for feature extraction and artificial neural networks for classification. ridgelet and curvelet transform [11] have been introduced. Sheeba et al. [12] proposed a method uses both Local Binary Pattern (LBP) to extract texture features and Learning Vector Quantization (LVQ) method for classification. The performance of iris recognition system depends on the good image quality and extremely clear iris texture details. Some attributes (contrast, brightness and existing noise) are highly sensitive to the specific characteristics of each image. Different lightening or camera properties can lead to images, for the same scene, have pixels' values very different with each other; these big differences would cause significant matching failure rates. Most of the existing iris recognition methods extract either the multi resolutional or the directional features of iris image. They may use Gabor filter or wavelet transforms (with two or four quantization levels) to establish the feature vector. This kind of features has robustness to contrast and illumination changes. These methods do not utilize a significant component of the rich discriminatory information available in the iris signatures.

Aim of this paper is to introduce a novel iris recognition method based on the gradient components distribution to extract iris features; the kind of these features is robust against the local illumination changes may appear in the iris image.

The set of used gradient based features consist of low order norms of the gradient components, this set can be considered as the complementary set to that introduced in our previous paper [13].

II. PROPOSED METHOD

Fig. 1 shows the layout of the proposed iris recognition method; it passes through many stages. The steps of these stages are described in the following sub-sections.

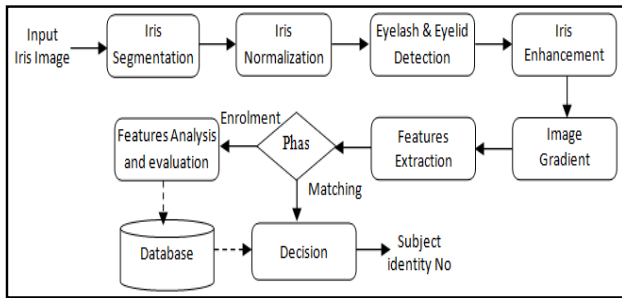


Fig. 1 Block diagram of the proposed system

A. Iris Segmentation

Iris segmentation is the process that is done to localize and extract the iris region from the other parts of the eye image. In our earlier method described in [14], a fast and accurate algorithm for detecting the boundaries between pupil and iris and between sclera and iris had been proposed. Original iris images may have low contrast and non-uniform illumination, caused by the position of the light source and this will impair the iris segmentation's process. Therefore, before applying this process, the iris image must be enhanced in order to get an image with uniformly distributed brightness and have better contrast; this brightness-contrast condition is handled by means of linear contrast stretching to bring the iris image into intensity range that is more normal or suitable to be segmented accurately. This iris enhancement step is just for segmentation purpose.

The introduced Iris boundaries localization algorithm implies the following steps:

Step 1. Is applied to determine the pupil geometrical parameters (i.e., center point coordinates & radius) from the enhanced iris image, the taken steps are:

- The histogram of the cropped area containing the iris region is determined. Then, the suitable threshold value is assessed from the histogram to segment the image into pupil (black) & non-pupil (white) regions.
- The seed fill algorithm is used to collect the largest black segment found in the image, and consider it as the initially collected pupil segment.
- The specular spot reflection (i.e., white) areas, which found in the pupil's segment, are removed by filling the whole pupil's area with black color.
- The coordinates of the center point and radius of the pupil's segment are determined, and consider them as the initial values for the pupil geometrical parameters.

- The circle fitting algorithm is applied to get more accurate values of pupil's center coordinates and radius.

Step 2. Allocate the iris outer boundary; our introduced method is based on using Leading Edge Detection method.

Fig. 2 shows samples of the detected iris regions when the developed method is applied on CASIA V4.0 images. The attained accuracy rate for localizing both the inner and outer iris boundaries as circles shape was 100% for CASIA v4.0-interval database images.

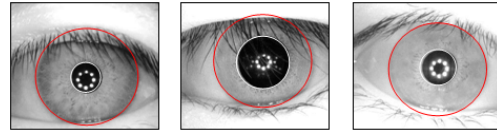


Fig. 2 Samples of iris localization results for CASIA v4.0-interval

B. Iris Normalization

The captured iris images can have different sizes; this variation is due to pupil dilation caused by varying levels of illumination, rotation of the eye and other factors. The normalization process will produce iris regions, which have the same constant dimensions. So, once the iris region is localized from the previous stage, the iris should be normalized and mapped to change the iris shape from circular to rectangular form. The size normalization and shape conversion is accomplished by unwrapping the iris region and map all the points lay between the iris boundaries from the original Cartesian coordinates $I(x, y)$ into their equivalent normalized polar coordinates $I(r, \theta)$ using the following mapping equation:

$$I(x(r, \theta), y(r, \theta)) \rightarrow I(r, \theta) \quad (1)$$

where, $r \in [R_p, R_i]$; R_p is the Pupil's radius, R_i is iris's radius and θ is angle $\in [0^\circ, 360^\circ]$, (see Fig. 3).

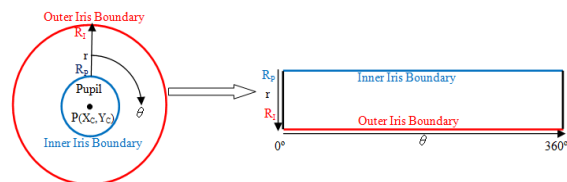


Fig. 3 Illustration of size normalization and mapping to rectangular shape of the iris region

The iris region is resembled to a rectangle of $(h \times w)$ pixels through making (h) samplings along radial (r) direction, and making (w) samplings along the whole angle θ range (i.e., $[0, 360]$), as shown in Fig. 4. The equations of applied normalization are the following:

$$x = X_p + r \sin(\theta) \quad (2)$$

$$y = Y_p - r \cos(\theta) \quad (3)$$

$$\text{Normalize_Iris}(i, j) = I(x, y) \quad (4)$$

where, $i = 0, 1, 2, \dots, h$, $j = 0, 1, 2, \dots, w, P(X_p, Y_p)$ is the pupil's center and $\theta = j \times (\pi / 180)$.

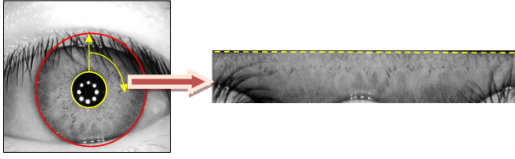


Fig. 4 Sample of normalization process output

In the conducted experiments, the size of the rectangular iris image is set (60, 360) pixels. Only the iris portion lay under the upper dotted line (see Fig. 4), was used to provide iris texture signature (i.e., features vector) for recognition purpose, the region lay above the upper dotted line mostly contains some pixels of pupil region because the pupil region is not perfectly circular.

C. Eyelashes and Eyelids Detection

Usually, in the iris image area the overlapped eyelashes points appear dark (as black) pixels, and they may locate at the upper and lower side of the image; while the overlapped eyelid points appear bright (as white) pixels. Also, it may appear at the upper and lower sides of the iris image. In this paper a method is proposed to detect the eyelid and eyelashes pixels, it consists of the following main steps:

Step 1. Generate an Initial Mask

The mask initialization is the important step to detect eyelash and eyelid as noisy points. The initial mask consists only of two regions: one taking as a noisy ($=0$) and the other as the iris ($=1$) through applying linear contrast stretching upon the iris image; this will shift the lowest existing gray level value toward 0, and the highest gray toward 255. In order to make this mapping process lead to stable eyelashes and eyelids detection performance, the lowest and highest gray level component values are assessed according to the following statistical bases:

$$V_{lowest} = M - a \sigma \quad (5)$$

$$V_{highest} = M + a \sigma \quad (6)$$

where V_{lowest} and $V_{highest}$ are the assessed values for the lowest and highest gray levels values for the iris pixels, M is the mean value for the image gray levels; (σ) is the corresponding standard deviation value and (a) is a predefined parameters used to control the strength of the stretching parameter, it value should be within the range [1, 3]. Then, the linear contrast stretching is done by applying the following mapping equation:

$$E_{img}(x,y) = \begin{cases} 0 & \text{if } I(x,y) < V_{lowest} \\ 255 \left(\frac{I(x,y) - V_{lowest}}{V_{highest} - V_{lowest}} \right) & \text{if } V_{lowest} \leq I(x,y) \leq V_{highest} \\ 0 & \text{if } I(x,y) > V_{highest} \end{cases} \quad (7)$$

where, $E_{img}(x,y)$ is the image after applying contrast stretching, and $I(x,y)$ is the original image.

Step 2. Apply Dilation and Erosion

Dilation and erosion are the most basic morphological operations. Both dilation and erosion are produced by the moving the structuring element or sub image around the image. Based on the image is to be dilated or eroded the size of the structuring element is choose, it is odd square matrix which contains binary elements that is 0's and 1's. After the step of marking the nominated eyelids and eyelashes as dark points, it can be noticed that some small clumps of noise points (0's) appears in the produced binary iris image, so dilation operation is used to remove these noise points from the iris region through replacing the mark of false assigned noise pixels to foreground pixel. Erosion is used to eliminate small clumps of iris points that appear in the noise region.

Step 3. Applying Seed Fill Algorithm

Perhaps iris mask, may be contain patch of noisy point (0's) appear in the interest region (iris), so, the seed fill algorithm remove like this patch through checks the value of the mask's pixels to the right, left, down and up of the current pixel, and it change any noise pixel value from zero to one and add it to the segment array.

D. Contrast Enhancement

Normalized iris image should be enhanced before features extraction, because these images may have low contrast and may have non uniform brightness due to the changes in position of light sources; these problems may significantly affect the following feature extraction and matching processes. Therefore contrast stretching is adopted to enhance the normalized iris image and to get an image with uniformly distributed brightness and have better contrast; the purpose of contrast stretching is to bring the iris image into an intensity range that is more normal or suitable for features extraction phase.

At first, the mean (M) and standard deviation (σ) of the normalized image are computed using the following equations:

$$M = \frac{1}{LxW} \sum_{i=0}^{255} i \times Hist(i) \quad (8)$$

where LxW is the image size, $Hist(i)$ is the total number of pixels in the i^{th} gray level.

$$\sigma = \frac{1}{LxW} \sum_{i=0}^{255} (i - M)^2 \times Hist(i) \quad (9)$$

The applied mapping function for contrast stretching can be found by the following equation:

$$G'(x,y) = \frac{A}{\sigma} (G(x,y) - M) + 128 \quad (10)$$

where, $G(x,y)$ is the pixel's intensity and $G'(x,y)$ is the mapped pixel value. The suitable value of (A) parameter is

assessed by testing. A sample of the enhancement process is shown in Fig. 5, mapping function will maps the minimum gray level in the image to zero and the maximum gray level to 255, the other gray levels are remapped linearly between 0 and 255.

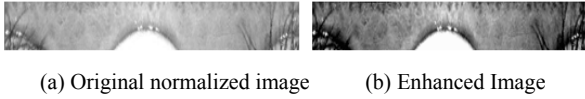


Fig. 5 Sample of Enhancement Process Results

E. Features Extraction

Every iris image has distinctive feature that makes it distinguishable from other. So, good iris features should have high discrimination power in terms of identifying the iris images. In this a new set of texture features is proposed. The involved steps for determining these features are:

Step 1. Apply local gradient operators on the iris pixels. Gradient operator measures the directional change of the pixel value; this first order degree of intensity change measure captures the local textural behavior of the iris signal. Each element of the gradient output arrays represents the change in intensity, along specific direction, at certain position in the original image. The gradient operators (G) of an image consist of the following operators:

$$G = \left\{ \frac{\partial f}{\partial h}, \frac{\partial f}{\partial v}, \frac{\partial f}{\partial d} \right\} \quad (11)$$

where, $\frac{\partial f}{\partial h}$ is the gradient along the horizontal direction, $\frac{\partial f}{\partial v}$ is the gradient along the vertical direction, and $\frac{\partial f}{\partial d}$ is the gradient along the diagonal direction. The implication of horizontal, vertical and diagonal directions is due to get the benefit of full range of directionality.

The gradient arrays (images) along the horizontal, vertical and diagonal directions are computed according to the following equations:

$$G_H(x, y) = A(x, y) - A(x + 1, y) \quad (12)$$

$$G_V(x, y) = A(x, y) - A(x, y + 1) \quad (13)$$

$$G_D(x, y) = A(x, y) - A(x + 1, y + 1) \quad (14)$$

After the determination of the 3 gradient arrays, then the Max and Min values of the corresponding gradient values (G_H , G_V and G_D) are determined and registered in the two arrays (G_{Max} and G_{Min}); the values of G_{Max} () are indicators to local dissimilarity, while the values of G_{Min} () are indicators to the local connectivity:

$$G_{Max}(x, y) = \text{Max}(G_H(x, y), G_V(x, y), G_D(x, y)) \quad (15)$$

$$G_{Min}(x, y) = \text{Min}(G_H(x, y), G_V(x, y), G_D(x, y)) \quad (16)$$

Fig. 6 shows examples of the gradient images. Eventually, any pixel has large gradient value, along any direction, is an edge pixels.

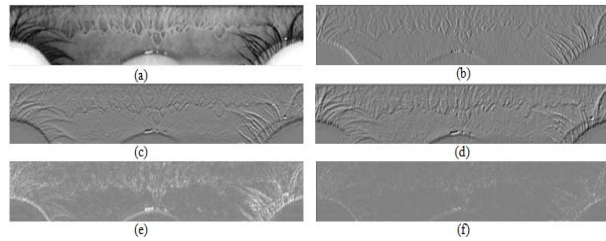


Fig. 6 Gradient images (a) iris image, (b) the horizontal gradient image, (c) the vertical gradient image, (d) the diagonal gradient image, (e) Max gradient, (f) Min gradient. The gray colored pixels indicate places have small gradient; while the black and white pixels indicate places have large gradient

Step 2. Partitioning the gradient image into overlapped blocks with certain overlapping ratio (O_{Ratio}) along the horizontal (x) and vertical (y) directions, as shown in Fig. 7. The number of blocks along the vertical (n_y) and horizontal (n_x) directions should predefined, then the block dimensions (h_{block}, w_{block}) in both directions are determined.

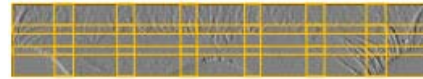


Fig. 7 Examples of partitioning the iris image into overlap blocks

Step 3. Determine Block Weight

After partitioning the gradient image into overlap blocking, these blocks are categorized into two classes: (i) iris blocks, (ii) noisy blocks, through applying the following criterion:

$$F = D_{Rate} (\mu - t) \quad (17)$$

$$w(\mu) = \frac{1}{1 + \exp(F)} \quad (18)$$

The suitable value of D_{Rate} and t parameters are assessed by testing, where, (μ) is the ratio of total numbers of flagged noise pixels (eyelash and eyelid) relative to the block size; the value of block decision weight $w(\mu)$ should be between the range [0, 1]. Fig. 8 presents three different iris blocks taken from different iris regions.

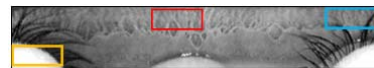


Fig. 8 Examples of three iris blocks taken from different iris regions (the block surrounded by red frame is purely iris, the region surrounding by cyan frame is partially contaminated, and the block surrounded by yellow frame is completely contaminated)

Mostly, the iris blocks located at middle region and nearest pupil take high weight values because these regions less affected by the noisy points of eyelashes and eyelids.

Step 4. In this step, the density (M_{GH} , M_{GV} , M_{GD}) of the horizontal, vertical and diagonal gradient components, respectively, are determined. Also, the average density values (M_{GMax} and M_{GMin}) are determined from the Max and Min gradient values, respectively. The density (norms) is calculated for each iris block separately, and then they assembled in one features vector to be treated as a signature vector for the iris image. The values of average density are calculated as iris features using the following equations:

$$M_{GC}(m) = \frac{1}{n_{iris}} \sum_{p(x,y) \in \text{block}} |G_C(x,y)|^m \quad (19)$$

$$M_{GC}^s(m) = \frac{1}{n_{iris}} \sum_{p(x,y) \in \text{block}} \text{sign}(G_C(x,y))^m \quad (20)$$

$$M_{Gmax}(m) = \frac{1}{n_{iris}} \sum_{p(x,y) \in \text{block}} |G_{Max}(x,y)|^m \quad (21)$$

$$M_{Gmin}(m) = \frac{1}{n_{iris}} \sum_{p(x,y) \in \text{block}} |G_{Min}(x,y)|^m \quad (22)$$

where G_C is either G_H , G_V or G_D ; n_{iris} is the number of iris points (p) belong to the block $n_{iris} = (h_{block} \times w_{block} - N_{NoisePoints})$; m is the order of the norm for the components (G_H , G_V , G_D), and $m = [0.5, 0.75, 1]$. The adoption of low order norms is due to the derived conclusion in our previous work; because it was noted that the discrimination power of high order norms is low and they are not useful for iris recognition task.

F. Determination of Features Templates

Before starting the matching process, the template feature vector T for each class (person) should be determined and registered in a database. For computing the template vectors for each class, the mean and standard deviation vectors for the feature vectors extracted from different image samples belong to one class are determined using the following equations:

$$\text{Mean}(f,c) = \frac{1}{NoSmp} \sum_{s=1}^{NoSmp} \text{Feature}(f,c,s) \quad (23)$$

$$\text{Std}(f,c) = \frac{1}{NoSmp} \sqrt{\sum_{s=1}^{NoSmp} (\text{Feature}(f,c,s) - \text{Mean}(f,c))^2} \quad (24)$$

where, the indices $f \in [1, NoFeatures]$, $c \in [1, NoClasses]$, $s \in [1, NoSamples]$; $NoSmp$ is the number of training samples for each class.

The adopted mechanism to handle the features analysis task was aimed to find out the lowest possible combination of features that can lead to good iris recognition results; the recognition accuracy was evaluated using the following measure:

$$\text{SuccessRate} = \frac{\text{No. of Successful Hits}}{\text{Total No. of Recognition Tests}} \quad (25)$$

In this work, the recognition accuracies for all features combinations have been tested. The tests started with single features (i.e., every feature is tested alone), then the number of features was expanded to pair of features (i.e., combinations consist of two features), then to triple features combination and more.

Then, the mean value (i.e., template values) and its associated standard deviation value for each feature belong to successful discriminating combinations are calculated for all classes, and the values are stored in a dedicated database.

G. Matching and Recognition Phase

For matching purpose, the famous four types of the weighted Euclidian distance measures [15] have been used to determine the similarity degree between the feature vectors (extracted from tested samples) with the template feature vectors (each of them representing certain class). The Euclidian distance measures are expressed mathematically as follows:

$$\text{WED}(S_i, T_j) = \sum_k |S(i).f(k) - T(j).f(k)| \times (S(i).w(\mu) \times T(j).w(\mu)) \quad (26)$$

$$\text{WED}(S_i, T_j) = \sum_k [S(i).f(k) - T(j).f(k)]^2 \times (S(i).w(\mu) \times T(j).w(\mu)) \quad (27)$$

$$\text{WED}(S_i, T_j) = \sum_k \left| \frac{S(i).f(k) - T(j).f(k)}{T(j).\sigma(k)} \right| \times (S(i).w(\mu) \times T(j).w(\mu)) \quad (28)$$

$$\text{WED}(S_i, T_j) = \sum_k \left[\frac{S(i).f(k) - T(j).f(k)}{T(j).\sigma(k)} \right]^2 \times (S(i).w(\mu) \times T(j).w(\mu)) \quad (29)$$

where, $S(i).f(k)$ is the value of k^{th} feature extracted from i^{th} sample and $T(j).f(k)$ is the template value of k^{th} feature belong to j^{th} class.

The distance measure provides a good way to test the strength of the feature vector (s) and it is required to assess the capability of recognizing and identifying persons.

III. RESULTS AND DISCUSSION

The performance of the proposed iris recognition is tested using CASIA v4.0-interval database; it consists of 2639 iris images captured from 249 subjects. The number of right iris images is 1332 images taken from 198 different subjects; the other 51 classes do not have any sample of right iris. While the left iris images are 1307 images belong to 197 subjects. One of the most important properties of iris, which makes it a wonderful biometric identification technology, is the "genetic independence"; i.e., iris not only differ between identical twins, but also between the left and right eye, so, in our conducted tests we have considered right and left iris as different classes belong to the same person (subject), so, the total number of classes will be 395 and number of processed images is 2639 images. Many researchers have applied the feature extraction stage only upon the iris images which are

correctly segmented and have sufficient texture information for recognition, while in our study the conducted tests have been applied on the whole CASIA v4.0-interval database images.

The suitable parameters values that led to highest successful recognition rates are shown in Table I. Equation (29) of the weighted Euclidian distance measure is adopted; because it had led to the highest recognition rate.

TABLE I
OPTIMUM PARAMETER'S VALUES

Parameter Name	Optimum Value
O_{Ratio}	0.1
h_{block}	14
w_{block}	45
Image height	60
Image width	360
NX	8
NY	4
Total number of blocks	32
A	100
D_{Rate}	20
t	0.6

The identification results for different types of features are listed in Table II; it shows the attained recognition success rates for CASIA v4.0 database, when only single, double, third, fourth features are used for representing each of the 32 iris block. The best single feature was $|M_{GV}(0.5)|$, because it led to recognition rate (91.97%); while the best combination of two features are $\{|M_{GV}(0.5)|, M_{GMin}(0.5)\}$ because it led to recognition rate (99.58%). The best recognition rate for combinations of three features $\{|M_{GV}(0.5)|, M_{GMin}(0.5)|, |M_{GH}(0.5)|\}$; it led to recognition rate (99.92%).

TABLE II
RECOGNITION RATES FOR CASIA V4.0 DATABASE

No. of Features	Features Type	Recognition Rate (%)
1	$ M_{GV}(0.5) $	91.97
2	$ M_{GV}(0.5) , M_{GMin}(0.5)$	99.58
3	$ M_{GV}(0.5) , M_{GMin}(0.5), M_{GH}(0.5) $	99.92
4	$ M_{GV}(0.5) , M_{GMin}(0.5), M_{GH}(0.5) , M_{GV}(0.5) $	99.92

Taking into consideration that the used images belong to CASIA v4.0-interval database are the same iris images belong to CASIA v3.0-interval database. The test results were obtained by running the developed iris recognition system on computer platform has 2.4 GHz Core i5 processor, 2 GB RAM, with Windows-7 OS platform. The programs have been developed using Visual Basic-6 programming language.

IV. CONCLUSIONS

In this paper, a novel method is proposed for iris recognition; it extracts the distinctive iris features based on the gradient components which are less susceptible to lighting, contrast and camera changes. For iris segmentation we have used our proposed method that mentioned in [14]. Then,

scaling and mapping operations have been carried out to produce a rectangular iris image that has a size (60 x 360 pixels). The overlapped eyelid and eyelash points (i.e., noise points), which may appear in the normalized iris image, have been detected carefully. By dividing the iris into overlapped blocks, some of these blocks are noise free, which produces accurate recognition when it compare with the enrolled blocks. This decreases the error rate in the recognition of noisy iris block in which the feature extraction and comparison for each of these blocks avoiding the noise points, that localized in some of the iris blocks (this type of noise caused by occlusion of eyelash or eyelid) which localized in the lower, left and right iris blocks. The adopted mechanism to handle the feature analysis task was aimed to find out the lowest possible combinations of features that can lead to good texture recognition results. The size of features combination was gradually increased and at each test step the best sets of features which can give the highest recognition rate found. In this paper, the sets of features combination was started with single feature and gradually expanded to a pair of features, and then to a set consist of triple and so on.

Image gradient components proved to be good iris texture descriptors because they determine the local directional variations along the iris image area. From the listed table it can be concluded that using the first order of gradient operator for iris signature formation gives reliable results up to 99.92 recognition rate for whole CASIA V4-Interval database images with small size of feature vector with using lower norm (0.5).

REFERENCES

- [1] J. W. Lewis, "Biometrics for Secure Identity Verification: Trends and Developments", M.Sc. Thesis, University of Maryland, Bowie State University, 2002. <http://acsupport/europe.umuc.edu/~meinkej/inss690/lewis.pdf>
- [2] J. Daugman, "The Importance of Being Random: Statistical Principles of Iris Recognition", Pattern Recognition Vol. 36, Pp. 279-291, 2003.
- [3] L. Ma, T. Tan, Y. Wang, and D. Zhang, "Personal Identification Based on Iris Texture Analysis", IEEE Trans. Pattern Analysis and Machine intelligence, Vol.25, No. 12, Pp. 1519-1533, 2003.
- [4] R. Wildes, "Iris Recognition: An emerging biometric technology," Proc. IEEE, Vol. 85, Pp. 1348-1363, 1997.
- [5] W. Boles, B. Boashah, "A Human Identification Technique Using Images of the Iris and Wavelet Transform," IEEE Trans. on Signal Processing, Vol. 46, No. 4, Pp. 1185-1188, 1998.
- [6] J. G. Daugman, "High Confidence Visual Recognition of Persons by a Test of Statistical Independence", IEEE Tans. Pattern Analysis and Machine Intelligence, Vol. 15, No. 11, Pp. 1148-1161, 1993.
- [7] D. Monro, R. Soumyadip and Z. Dexin, "DCT-based Iris Recognition", IEEE. Trans. Patt. Anal. Mach. Intell., Vol. 29, Pp. 586-595. DOI:10.1109/TPAMI.2007.1002, 2007.
- [8] A. Azizi and H. R. Pourreza, "Efficient IRIS Recognition through Improvement of Feature Extraction and Subset Selection", International Journal of Computer Science and Information Security (IJCSIS), Vol. 2, No.1, 2009.
- [9] S. Lim, K. Lee, O. Byeon and T. Kim, "Efficient Iris Recognition through Improvement of Feature Vector and Classifier", ETRIJ, Vol.23, No.2, Pp. 61-70, 2001.
- [10] A. M. Sarhan, "Iris Recognition Using Discrete Cosine Transform and Artificial Neural Networks," Journal of Computer Science vol. 5 (5), Pp. 369-373, 2009.
- [11] N. Najafi and S. Ghofrani, "Iris Recognition Based on Using Ridgelet and Curvelet Transform", Int. J. Signal Process Image Process Pattern Recognition, Vol.4, No.2, Pp. 7-18, 2011.

- [12] S.J. Sheeba, S.S. Jeya, S. Veluchamy, "Security System Based on Iris Recognition", Research Journal of Engineering Sciences, Vol. 2, No. 3, Pp. 16-21, 2013.
- [13] I. A. Saad and L. E. George, "Iris Recognition Based on the Spatial Density Distribution of the Gradient Components," unpublished.
- [14] I. A. Saad and L. E. George, "Robust and Fast Iris Localization Using Contrast Stretching and Leading Edge Detection", International Journal of Emerging Trends & Technology in Computer Science (IJETTCS), Vol. 3, Pp. 61-67, 2014.
- [15] M. G. Thomason and R. C. Gonzalez, "Syntactic Pattern Recognition", Publisher: Westview Press, 1978.